CrossMark

ARTICLE

Carbon-doped titania as a precursor for titanate nanotubes

Uta Helbig[a)]
Department of Materials Engineering, Technische Hochschule Nuremberg Georg Simon Ohm, Nuremberg D-90489, Germany; and Institute for Chemistry, Materials and Product Development OHM-CMP, Technische Hochschule Nuremberg Georg Simon Ohm, Nuremberg D-90489, Germany

Kai Herbst
Department of Materials Engineering, Technische Hochschule Nuremberg Georg Simon Ohm, Nuremberg D-90489, Germany

Jewgeni Roudenko
Department of Materials Engineering, Technische Hochschule Nuremberg Georg Simon Ohm, Nuremberg D-90489, Germany; and Institute for Chemistry, Materials and Product Development OHM-CMP, Technische Hochschule Nuremberg Georg Simon Ohm, Nuremberg D-90489, Germany

Jens Helbig
Institute for Chemistry, Materials and Product Development OHM-CMP, Technische Hochschule Nuremberg Georg Simon Ohm, Nuremberg D-90489, Germany

Bastian Barton and Ute Kolb
Institute of Inorganic Chemistry and Analytical Chemistry, Johannes Gutenberg University Mainz, Mainz D-55128, Germany

(Received 1 October 2017; accepted 16 February 2018)

Carbon-doped titania was fabricated via carbothermal treatment in nitrogen–acetylene gas flow and further used as a precursor for multiwalled titanate nanotube (TNT) synthesis via alkaline hydrothermal route. Investigation of the reaction products after hydrothermal treatment of carbon-doped titania using Transmission electron microscopy, X-ray diffraction, and Brunauer–Emmett–Teller method shows the successful formation of TNTs. The presence of carbon was proved although the type of incorporation could not be certified. All samples show approximately the same carbon content before and after hydrothermal treatment. An increasing pretreatment temperature of titania precursor powders yields more secondary products in the nanotube samples, indicating lower reactivity of the titanium oxycarbide phase during hydrothermal treatment. In this study, TNTs with 6 wt% carbon and with the highest specific surface area of 340 m^2/g were formed via hydrothermal treatment of carbon-doped titania precursor powder exposed to 700 °C during carbothermal pretreatment.

I. INTRODUCTION

Nanotube structures are known for various materials including titanium oxide. Tubular titanium oxide-based nanostructures are interesting for many applications such as energy storage and conversion, photocatalysis, and hydrogen storage. Their dominant characteristic is the high specific surface area. Depending on the application, the material can be modified enabling electrical conductivity or catalytic activity.[1–6] Two methods for the fabrication of titanium oxide-based nanotubes are described in the literature: anodic oxidation and hydrothermal treatment. Anodic oxidation[7] yields single-walled titania nanotubes which form highly ordered arrays. Metallic titanium foils are oxidized in a two-electrode arrangement at constant potential at room temperature. Ethylene glycol containing NH_4F and H_2O is used as electrolyte, and typical voltages during anodic oxidation are 40–60 V. The anodization process leads to tubular structures with diameters of about 100 nm, which are oriented perpendicular to the surface of the titanium foil. The specific surface area thus obtained is about 40 m^2/g. Due to the oriented arrangement of the tubes, potential applications mainly as filter material are discussed. For that reason, the aim of many research activities is to increase the length of the tubes, i.e., the thickness of the array, to achieve stable free-standing membranes.

Alkaline hydrothermal treatment[8,9] yields multiwalled titanate nanotubes (TNTs) with much smaller dimensions. The tubular structures are of snail type with typical inner diameters of about 3–10 nm. The length of the nanotubes is between 0.2 and 500 μm. Due to the small dimensions, high specific surface area is obtained. Values up to 478 m^2/g were observed.[10] Several types of modification of the nanotubes are proposed in the literature to add functionalities. An

a)Address all correspondence to this author.
e-mail: uta.helbig@th-nuernberg.de
DOI: 10.1557/jmr.2018.49

 © Materials Research Society 2018

https://doi.org/10.1557/jmr.2018.49 Published online by Cambridge University Press

important example is the decoration with nanoparticular catalysts.[11]

For the application as the electrode material in fuel cells or batteries, beside high specific surface area, high electrical conductivity is required. Pure TNTs have a conductivity of $\approx 10^{-8}$–10^{-6} S/cm due to their semiconducting nature[12,13] which is not sufficient for the application as the electrode material. To increase the electrical conductivity of titania nanostructures, successful doping with carbon via carbothermal treatment in reducing atmosphere (acetylene–nitrogen) was reported in Refs. 14–17. The authors describe the formation of single-walled titania nanotubes via self-organizing electrochemical anodization and subsequent calcination. The nanotubes have a diameter of 100 nm and are of anatase phase. After mild carbothermal treatment at 500 °C in nitrogen–acetylene gas mixture, the nanotubes are doped with carbon, which was proved by photocurrent measurements.[15] Above 600 °C, the formation of substoichiometric titanium oxides (suboxides), titanium oxycarbides, and titanium carbide (TiC) occurs.[18] In comparison, when commercial TiO_2 powders (Aeroxide® TiO_2 P25 Evonik Industries AG, Essen, Germany) are carbothermally treated in nitrogen–acetylene gas mixture, a significant increase of electronic conductivity is observed.[16]

However, the carbothermal treatment cannot be directly transferred to nanotube material synthesized via the hydrothermal method due to the low thermal stability of protonated TNTs.[19] The as-synthesized TNTs contain a high amount of sodium cations, which are exchanged for protons during post-processing. In the protonated form, the nanotube material is stable only up to 200–300 °C. Significant loss of the specific surface area[20] or even the collapse of the tube morphology[21] is observed upon calcination above 300 °C. For that reason, posttreatment of TNTs with different carbon sources leads to rather low specific surface areas or even the loss of tubular morphology. For example, Wu et al. synthesized protonated TNTs via the hydrothermal method. After drying, the nanotubes were treated in ethanol vapor and subsequently calcined at 400 °C in nitrogen atmosphere, leading to single-walled carbon-doped TiO_2 nanotubes of anatase phase with the specific surface area of 146.3 m^2/g. The carbon content was not reported.[22] Furthermore, Ansón-Casaos et al. mixed protonated TNTs ($\approx$300 m^2/g) with different amounts of glucose and calcined the mixtures at 410 °C in nitrogen atmosphere. The resulting products were solid titania nanorods of anatase phase with a carbon content in the range of 0.3–25.4 wt% and a specific surface area in the range of 99–237 m^2/g. Besides carbon doping, accumulation of porous carbon on the nanorod surface was detected for carbon contents above 5 wt%, leading to an increased specific surface area.[23] Therefore, a different carbon doping approach is needed to increase the electrical conductivity of TNTs while maintaining the high specific surface area.

It was shown that carbon is retained in titanium oxide-based nanotubes and nanowires after hydrothermal treatment when carbon-doped TiO_2 precursors are used.[24–26] Xu et al. obtained carbon-doped TiO_2 via sol–gel method and synthesized TNTs via the hydrothermal method. After calcination at 500 °C, carbon-doped TiO_2 nanotubes of anatase phase were formed. The slightly increased electrical conductivity, detected by impedance spectroscopy, was ascribed to carbon in the TiO_2 nanotubes. The carbon content was not reported. Goriparti et al. describe a multistep process to obtain carbon-doped nontubular TiO_2-(B) nanowires. First, TiC is thermally oxidized in air to form carbon-doped TiO_2, which is subsequently converted into carbon-doped titanium oxide nanowires via alkaline hydrothermal treatment. After calcination at 300 °C, the carbon-doped TiO_2-(B) nanowires are formed. Impedance spectroscopy shows a slight increase of electrical conductivity ascribed to carbon presence in the nanowires. However, the authors could only prove the increase of incorporated carbon compared to a reference sample.

The publications mentioned above show that a reducing atmosphere and rather high carbon content seem to be crucial to significantly increase the electrical conductivity of titania nanostructures but cannot be applied to protonated TNTs, due to their low thermal stability.

Hence, the aim of our study is to examine a different approach. The focus of our investigations was to analyze whether TiO_2 powders, carbothermally pretreated in reducing atmosphere, can be converted into carbon containing TNTs via hydrothermal treatment. Of particular interest is the correlation between the carbon content in precursor powders prior to and in the products after the hydrothermal treatment in dependence of the carbothermal pretreatment parameters.

II. EXPERIMENTAL

A. Carbothermal treatment of titania powders

The samples were treated carbothermally in acetylene/nitrogen flow.[17] A prototype reactor was used consisting of tubular heating elements which were thermally insulated from the environment. The length of the heated zone was 3 cm. The powder was inserted as uniaxially pressed cylinders in an alumina tube with an inner diameter of 6 mm. Thermocouples were inserted into the powder sample as well as in the heating elements. The reactive gas was passed directly onto the sample to ensure that the powder is flowed through.

Titania powder samples were treated in acetylene/nitrogen flow (10/90 vol%) of 0.3 L/min at 700 °C, 800 °C, 900 °C, 950 °C, 1000 °C, and 1050 °C for 10 min with a heating and cooling rate of 50 and 25 K/min, respectively. During heating and cooling, the acetylene–nitrogen flow was 0.1 L/min. After carbothermal treatment, the samples were denoted as "CP" with

https://doi.org/10.1557/jmr.2018.49 Published online by Cambridge University Press

a following number describing the treatment temperature divided by 100. For example, "CP-9.5" represents a carbothermally treated titania powder at 950 °C. "CP-0" stands for an untreated titania sample.

B. Hydrothermal treatment

All samples are based on titanium dioxide powder by Evonik industries (Aeroxide® TiO_2 P25 Evonik Industries AG, Essen, Germany ≥99.5% purity). The powder typically has a specific surface area of about 50 m^2/g and consists of anatase and rutile with crystallite sizes of about 21 nm (more details on the raw materials can be found in the Supplementary Material). In the following, the untreated sample powder is denoted as CP0 and CP7-CP10.5 for carbon-treated samples. CP0 or carbon-doped titania powders (CP7-CP10.5) are converted into TNTs via hydrothermal treatment. 1 g of powder was dispersed in 325 mL deionized water and the suspension was ultrasonically treated for 15 min under magnetic stirring. In the following step, 160 g sodium hydroxide (NaOH, Carl Roth GmbH & CO. KG, Karlsruhe, Germany ≥99% purity) was added. The suspension was hydrothermally treated for 20 h under stirring (500 rpm) in an open PTFE flask with a magnetic stirrer, placed into a silicone oil bath (115 °C) and connected to an empty wash bottle via silicone hose. Subsequently, the suspension was washed with deionized water until the conductivity of the filtrate fell below 20 μS/cm. Subsequently, sodium ions were exchanged for protons via leaching in 0.1 M HCl for 15 min under stirring with a magnetic stirrer. The material was washed with deionized water until the conductivity of the filtrate was below 4 μS/cm. Ion exchange was confirmed by XRF measurements revealing a sodium content below 0.1 at.%. The suspension was vacuum-filtrated and the resulting powder was dried at 60 °C for 24 h in air. The obtained nanotube samples were denoted based on the precursor powder used during hydrothermal treatment, with the addition of "-NT". For example, "CP9.5-NT" stands for the nanotube sample that was synthesized from carbothermally treated titania "CP9.5" precursor powder.

C. X-ray diffraction

X-ray diffraction (XRD) patterns were recorded with a laboratory powder diffractometer XpertPro (PANalytical, Almelo, Netherlands) using Cu $K_{\alpha 1/2}$ radiation. The samples were prepared on 20-mm sample holders by back-loading method without further treatment. The diffraction patterns were taken in an angle range of 5–100° 2θ using a PIXcel detector (PANalytical, Almelo, the Netherlands). The nominal step size was set to 0.013°, and the time per step was 13.77 s. Qualitative phase analysis was performed using HighScore Plus (PANalytical, Almelo, the Netherlands). Quantitative phase content was determined via Rietveld refinement using PowderCell 2.4 (Federal Institute for Materials Research and Testing, Berlin, Germany).

D. Specific surface area (BET method)

The specific surface area was determined via the Brunauer–Emmett–Teller method (BET) using a NOVA 2200 Quantachrome apparatus (Boynton Beach, FL). The samples were dried at 150 °C for 60 min under vacuum prior to measurement. The adsorption–desorption isotherms were measured at 77 K with liquid nitrogen.

E. Scanning electron microscopy

Scanning electron microscopy (SEM) images were taken with a LEO 1525 (Carl Zeiss NTS GmbH, Oberkochen, Germany). The samples were mounted on double-side carbon tape and sputtered with carbon.

F. Thermogravimetry

The water and carbon content of all samples was investigated by thermogravimetric analysis (TGA). TGA was performed using a TG Iris F1 (Netzsch Geraetebau, Selb, Germany). Open alumina crucibles were used. The sample amount was 10–20 mg. The measurements were conducted with synthetic air. The reaction products were analyzed with a coupled FT-IR spectrometer (Tensor 27, Bruker Optics, Billerica, MA).

Earlier investigations showed mass gain during measurement, which occurs due to oxidation of titanium suboxide phases present in carbothermally treated samples above 800 °C. The mass gain overlaps with the mass loss due to oxidation of incorporated carbon impeding accurate measurement of carbon content. For that reason, all samples were pretreated with H_2O_2 to oxidize titanium suboxides prior to measurement.

The samples were treated in 60 vol% H_2O_2 for 15 min and dried at 60 °C in air for 24 h.

G. Transmission electron microscopy

Nanotube samples were prepared from washed and dried powder on carbon-coated Transmission electron microscopy (TEM) grids. TEM imaging was performed using a FEI TECNAI F30 S-TWIN transmission electron microscope (Thermo Fisher Scientific Inc., Waltham, Massachusetts) equipped with a field emission gun and working at 300 kV. TEM images were recorded with a CCD camera (16-bit 4096 × 4096 pixel GATAN ULTRASCAN4000, Roper Technologies, Inc., Sarasota, Florida) and acquired by Gatan Digital Micrograph software. TEM in-line holography was realized by focal series reconstruction from image series recorded using the FEI TECNAI F30 S-TWIN as described above, without aberration corrector, under suitable high-resolution TEM conditions. 40 images were recorded

https://doi.org/10.1557/jmr.2018.49 Published online by Cambridge University Press

at a primary magnification of 790,000 with 3-nm focal increment, thus covering a focal range of 114 nm including Gaussian focus. The accumulated dose per focal series was 168 $e^{-}/Å^2$. The images were hardware-binned by 2, followed by an additional software binning by 2 resulting in a physical pixel size of 0.0576 nm. After image alignment, an area of interest was chosen for exit wave reconstruction, employing a Gerchberg–Saxton algorithm implemented in Python. Residual axial aberrations were corrected by an automated minimization routine also implemented in Python.[27]

III. RESULTS

A. Undoped TNTs

As a reference material, undoped TNTs were synthesized via the hydrothermal route. Synthesis parameters were optimized in earlier experiments[19] and are given in the experimental section. Criteria for optimization were specific surface area, amount of nontubular by-products, and morphology. SEM investigations (data not shown) revealed that the nanotubes are strongly bundled. Appropriate adjustment of solid content during hydrothermal treatment minimized the amount of by-products which were identified as residual precursor powder.

Higher temperatures and longer treatment time resulted in the formation of nanofibers.

Figure 1 shows a TEM micrograph of the sample CP0-NT synthesized using the optimum parameters for hydrothermal treatment. The micrograph proves the tubular structure and illustrates the multiwall character of the nanotubes, which are strongly bundled. The inner diameter of the nanotubes is about 5 nm. BET measurements of the sample revealed a specific surface area value as high as 380 m^2/g.

The synthesis parameters were transferred to the hydrothermal treatment of carbon-doped precursor powders. The results were compared to the undoped TNTs.

B. Carbothermally pretreated precursor powder

To obtain the carbon-doped precursor powder, pure titania powder was carbothermally treated in acetylene/nitrogen flow following the parameters given in the experimental section. The resulting powder was characterized regarding morphology, carbon content (measured by weight loss), phase content, and specific surface area.

C. Thermogravimetry

The TGA curves for untreated pure titania (CP0) samples and powders carbothermally treated at different temperatures in nitrogen/acetylene flow are depicted in Fig. 2. All samples show an initial weight loss due to adsorbed water. The pure titania sample shows no further change during measurement. By contrast, all carbothermally treated powders show significant mass loss upon heating (samples CP7-10.5). The decrease starts at a temperature of about 380 °C, which corresponds to carbon starting to disintegrate. The reaction products were investigated with coupled FT-IR spectroscopy. The spectra showed the presence of carbon dioxide and carbon monoxide (Fig. S1). Thus, the mass loss occurring after 380 °C was ascribed to carbon. All thermogravimetry curves reach a plateau at high temperature. The weight difference between the end value and the mass level after initial water loss was used to determine the carbon content of the samples.

The carbon content of the carbothermally pretreated samples is between 8.9 and 44.3 wt%. Individual values are given in Table II. The amount of carbon incorporated in the powders increases with the reaction temperature

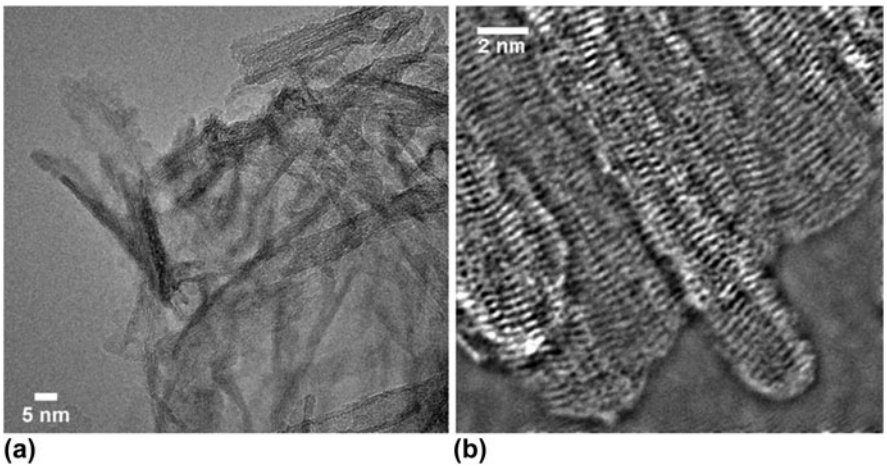


FIG. 1. TEM micrographs of TNTs obtained via hydrothermal treatment of titania powder (P25) at 115 °C for 20 h in NaOH solution. (a) Bundle of TNTs (CP0-NT) and (b) detailed TEM micrograph showing the tube walls.

https://doi.org/10.1557/jmr.2018.49 Published online by Cambridge University Press

applied during carbothermal treatment. The values rise up to a pretreatment temperature of 900 °C, from which it is nearly constant for higher temperatures.

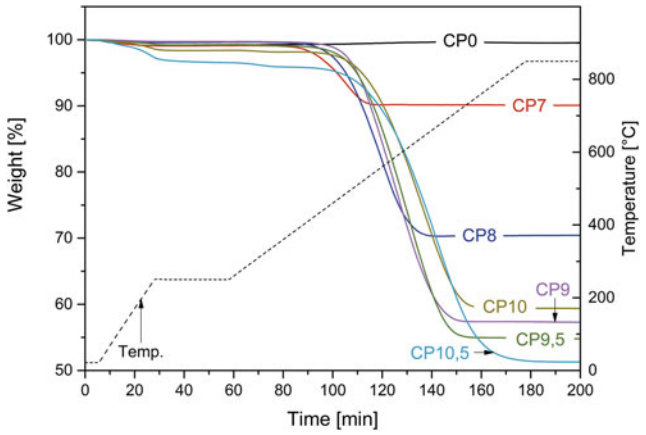


FIG. 2. Thermogravimetry curves for titania samples treated in nitrogen/acetylene flow at 700–1050 °C. The result for untreated powder is shown as a reference ("CP0") (modified after[19]).

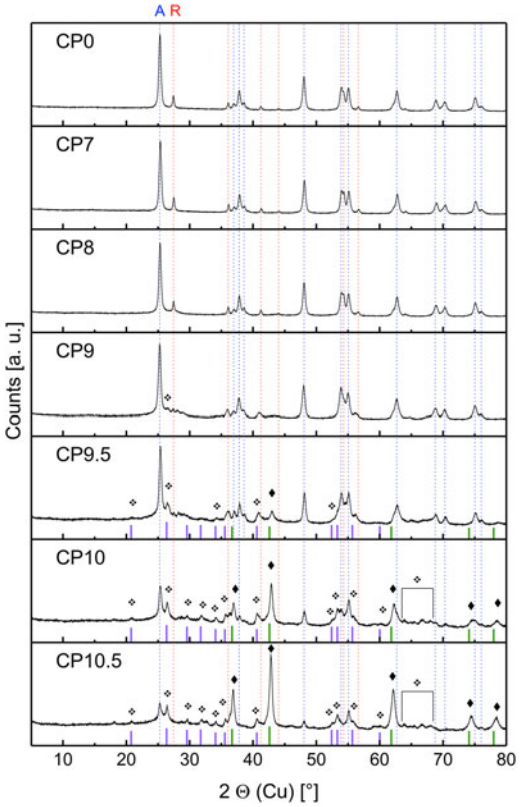


FIG. 3. XRD patterns of titania powders before (CP0) and after carbothermal treatment at temperatures in the range of 700–1050 °C (CP7-10.5). The lines represent peak positions from ICSD database (PDF-No.). A (blue dashed): anatase-TiO_2 (00-021-1272); R (red dashed): rutile-TiO_2 (00-021-1276); ♦ (green): titanium oxycarbide $TiC_{0.6}O_{0.4}$ as reported in Ref. 28; ❖ (pink): superimposed peaks of several Ti_nO_{2n-1} phases (color online, see the Supplementary Material for full patterns, modified after[19]).

D. XRD

The phase content of the carbothermally treated powders was investigated using XRD (Fig. 3). For comparison, the untreated titania powder P25 (CP0) was characterized regarding qualitative and quantitative phase content. The measurements reveal that the sample CP0 is a mixture of anatase and rutile. Quantitative phase analysis via Rietveld refinement further reveals an anatase content of about 88 vol% (Fig. S2).

Comparing the diffraction patterns of the undoped reference sample and the powders treated carbothermally at temperatures below 900 °C, it is noteworthy to mention that the phase content does not change significantly. Higher pretreatment temperatures induce phase transition from anatase and rutile to substoichiometric titanium oxides. From the suboxide series only Ti_9O_{17}, Ti_4O_7, and Ti_3O_5 could be detected depending on the pretreatment temperature. Detailed plots including all reference lines can be found in the Supplementary Material (Figs. S5–S8). The formation of suboxides starts with Ti_9O_{17} after pretreatment at 900 °C. At 950 °C and higher temperatures, Ti_3O_5 and Ti_4O_7 are observed. Above 900 °C, the reducing atmosphere during carbothermal treatment leads to the formation of titanium oxycarbides from the solid solution TiO–TiC. The anatase phase is present in all samples. Rutile is not detected after treatment at 950 °C and higher temperatures.

E. BET and SEM

The results of BET measurements and SEM investigations of carbothermally treated powder and untreated commercial P25 titania powder (CP0) were compared. Typical specific surface area values of untreated powder are in the range of 50 m^2/g. The sample shows the typical morphology showing larger agglomerates consisting of smaller primary particles. The SEM image is part of the Supplementary Material (Fig. S9).

Carbothermal treatment of the titania powder does not change the morphology and the specific surface area significantly. After treatment at 700 °C up to 900 °C (CP7-CP9), the specific surface area is about 55 m^2/g. Higher temperatures lead to a small decrease in the specific surface area down to 45 m^2/g. The values are supported by the SEM analysis, where no significant agglomeration or sintering effects can be observed (Fig. 4).

F. Carbon-doped TNTs from carbothermally pretreated powder

1. Thermogravimetry and specific surface area (BET)

Nanotubes were synthesized via the hydrothermal route from the pretreated carbon containing titania

https://doi.org/10.1557/jmr.2018.49 Published online by Cambridge University Press

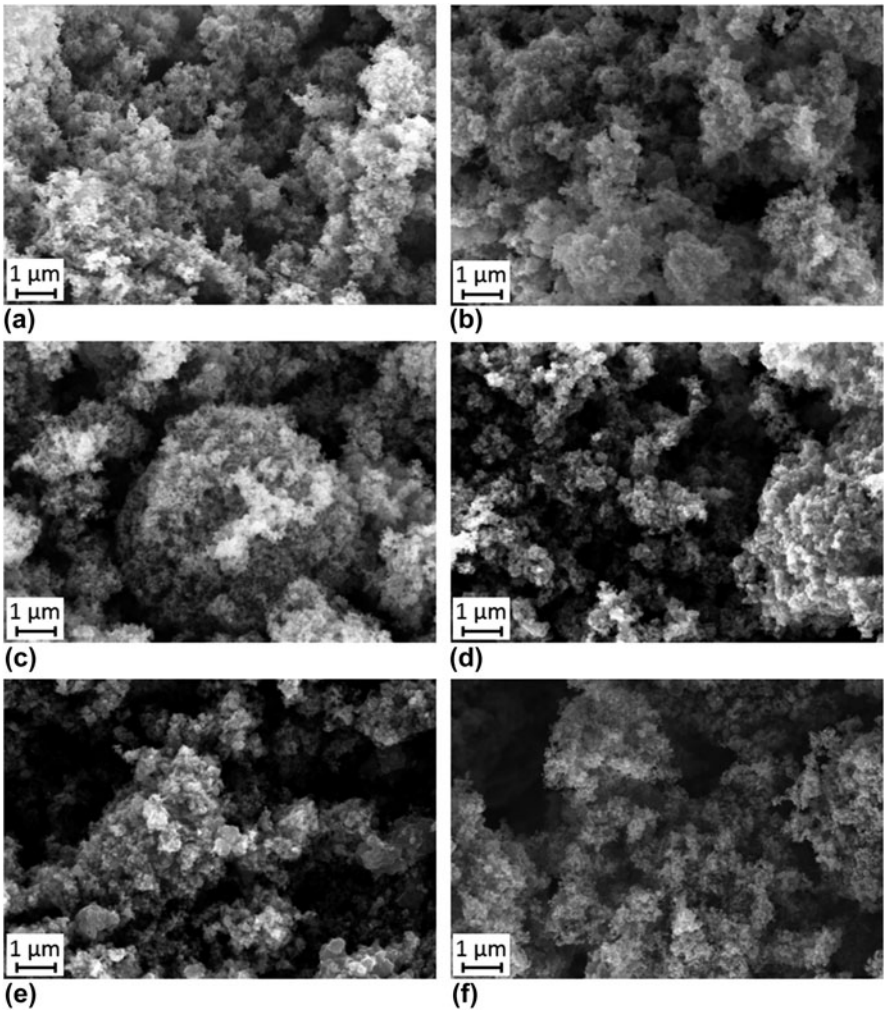


FIG. 4. SEM micrographs of carbothermally treated titania powders at 700–1050 °C. (a) CP7—52 m^2/g, (b) CP8—54 m^2/g, (c) CP9—55 m^2/g, (d) CP9.5—45 m^2/g, (e) CP10—45 m^2/g, and (f) CP10.5—48 m^2/g. (modified after[19]). For the micrograph of untreated titania powder (CP0), see Fig. S9.

powders using the optimized parameters as described above. The TGA of nanotube samples shows again initial mass loss in the temperature interval between 100 and 380 °C (Fig. 5). The corresponding analysis of degradation products revealed desorption of water. The comparison of the values of weight loss in the initial state for powders (Fig. 2) and tubular samples demonstrates that the tubes adsorb a higher amount of water indicating high specific surface area.

Between 380 and 700 °C further mass loss occurs, which is in analogy to the powder samples correlated with the degradation of incorporated carbon. The degradation products were analyzed using coupled FT-IR spectroscopy and were again identified as carbon monoxide and carbon dioxide.

Similar to the observations from the thermogravimetry of the powder samples, the undoped tube sample shows initial mass loss due to adsorbed water. After that no

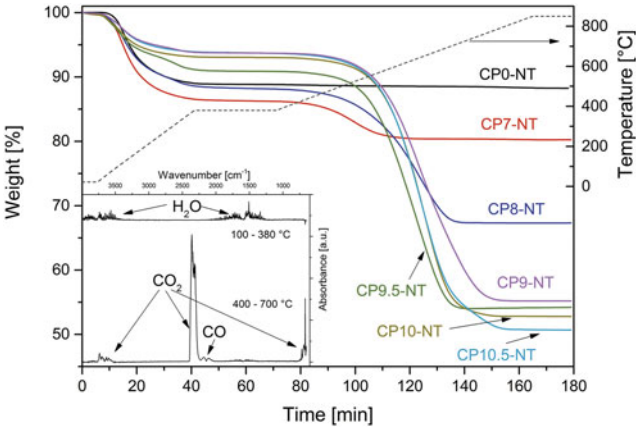


FIG. 5. TGA of TNTs (CP7NT–CP10.5-NT) synthesized from carbon-doped titania powders (CP7-10.5). CP0-NT was synthesized from undoped titania powder (CP0). The inset shows the corresponding FTIR spectrum of the measured exhaust gases (modified after[19]).

https://doi.org/10.1557/jmr.2018.49 Published online by Cambridge University Press

further change in the TG curve is observed. All samples synthesized from carbothermally treated precursor powders show additional weight loss indicating the incorporation of carbon in the material. The values for adsorbed water and incorporated carbon were again calculated based on the difference between initial values and plateaus after loss of water and weight constancy at 800 °C.

The amount of mass loss referred to water and carbon is correlated with the parameters for the pretreatment of the precursor powder. With increasing pretreatment temperature of titania powders (CP7-10.5), the carbon content in nanotube samples CP7-NT–CP10.5-NT increases from 6.0 to 43.5 wt%, whereas the amount of adsorbed water decreases from 13.6 to 6.2 wt% (see Table I).

The specific surface area of the samples after hydrothermal treatment is also dependent on the temperature of pretreatment of the precursor powders. The values do not reach the reference value of the undoped sample and decrease with increasing precursor powder treatment temperature (see Table I). The amount of adsorbed water correlates with the values for the specific surface area.

2. XRD

Powder diffraction patterns (Fig. 6) were taken from TNTs synthesized from carbothermally pretreated powders (CP7-10.5) and from undoped titania powder (CP0) for comparison. As expected, the undoped sample (CP0-NT) shows the typical diffraction pattern for TNTs as reported by various authors.[9,22,29,30] The XRD patterns are characterized by broad peaks. Peak positions, intensities, and widths may differ due to various hydrothermal syntheses and post treatment procedures. In Fig. 6, the peak positions commonly observed for TNTs are marked: ~10°, ~25°, ~34°, ~38°, ~44°, ~48°, ~60°, and 62°. The crystal structure of TNTs is widely discussed, but the layered $H_2Ti_3O_7$ monoclinic titanate structure is accepted by most authors.[10]

The diffraction patterns from nanotube samples fabricated from powders pretreated at 700–900 °C (CP7-NT–CP9-NT) show no significant difference to patterns from the undoped nanotube material. Closer inspection reveals triple peaks around 10° for the samples CP7-NT and CP8-NT. Additionally, the peak at ~34° is more pronounced.

Peaks at ~10° are ascribed to the interlayer distance between tube walls. Splitting into various peaks indicates more than one population of nanostructures having different interlayer distances. Fitting the peak positions of the CP7-NT and CP8-NT patterns leads to estimated d-values of 1.1, 0.9, and 0.8 nm. The interlayer distances allow the correlation with nanotubes, nanosheets, and nanoribbons. The peak splitting points toward nontubular but elongated by-products which are frequently observed and were investigated in detail by Papa et al.[31]

The diffraction patterns from samples synthesized from precursor powders treated at higher temperatures than 700 °C show better signal-to-noise ratio and new Bragg reflections with smaller FWHM, indicating additional crystalline phases. Starting with the pretreatment temperature of 800 °C, additionally to the nanomaterial, crystalline phases are observed. Anatase reflections can be found for all samples, most distinct at 950 and 1000 °C. Rutile is detected at 800, 900, and 950 °C and disappears for higher pretreatment temperatures. Titanium oxycarbides are found in the tube samples synthesized from powders carbothermally treated at 1000 and 1050 °C.

The typical nanotube pattern is suppressed for higher temperatures. However, the characteristic peaks at ~10°, a shoulder to the anatase peak at 25°, and the highest peak at 48° 2θ remain visible.

3. SEM

SEM images of samples after hydrothermal treatment of carbon-doped precursor powders are depicted in Fig. 7. All images show elongated structures beside agglomerated powder particles. The observations correspond to the results from specific surface area analysis and XRD. Although the investigations allow no quantitative interpretation, all samples seem to contain nanotubes, nanosheets, or nanowires. Particular by-products seem to be more pronounced for higher pretreatment temperatures. For samples synthesized from precursor powders treated at higher temperatures, slight coarsening of byproduct particles is observed.

TABLE I. Water and carbon content and specific surface area of undoped TNTs (CP0-NT) and carbon-doped TNTs (CP7-NT–CP10.5-NT), synthesized from untreated titania (CP0) and carbothermally treated titania powders (CP7-10.5), respectively.

Sample	CP0-NT	CP7-NT	CP8-NT	CP9-NT	CP9.5-NT	CP10-NT	CP10.5-NT
Temperature [°C]	...	700	800	900	950	1000	1050
C content [wt%]	0	6.03	20.91	36.7	40.27	43.09	43.53
H_2O content [wt%]	11.18	13.62	11.71	8.87	6.71	6.17	6.19
Specific surface area [m^2/g]	380	340	255	246	197	187	175

https://doi.org/10.1557/jmr.2018.49 Published online by Cambridge University Press

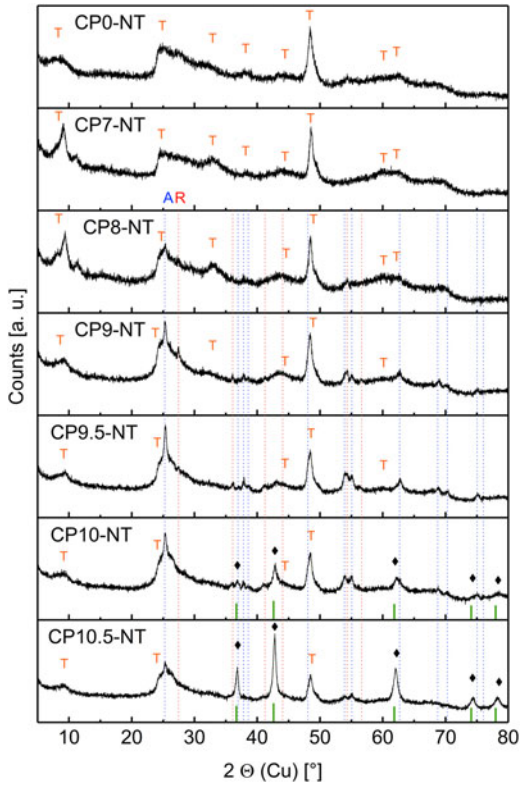


FIG. 6. Patterns of carbon-doped TNTs (CP7-NT–CP10.5-NT) and undoped TNT sample (CP0-NT). The lines represent peak positions from ICSD database (PDF-No.). A (blue dashed): anatase-TiO_2 (00-021-1272); R (red dashed): rutile-TiO_2 (00-021-1276); ◆ (green): titanium oxycarbide $TiC_{0.6}O_{0.4}$.[28] T: characteristic positions for TNTs (color online, modified after[19]).

EDX investigations were performed in several characteristic regions of the sample to investigate the chemical composition focusing on information about the carbon content. Parts consisting predominantly of elongated structure and agglomerated powder were selected for measurements.

The measurement at the 700 °C sample in a region containing predominantly nanotubes reveals carbon, titanium, and oxygen. The same elements were detected in the powder region. The relative peak intensities suggest that the relative amount of carbon is higher in the particle fraction. Note that the samples were sputtered with carbon to achieve sufficient conductivity for SEM analysis. For that reason, carbon can be expected on the whole sample. Analogous investigations at the sample synthesized from the powder pretreated at 1000 °C show similar results. All parts of the sample contain titanium, oxygen, and carbon. The highest relative amount of carbon is detected in a region where coarsened particles are observed. Parts of the sample consisting of finer powder show a lower amount of carbon. Intermediate values are measured at platelet structures. Single elongated structures were too narrow to perform selective EDX measurements.

4. TEM

The nanotube sample (CP7-NT) obtained from carbon-doped titania powder (CP7) pretreated at 700 °C was investigated using TEM (Fig. 8). The phase image of the TEM exit wave reconstruction proves that tube morphology was obtained via hydrothermal treatment of carbon-doped titania powders. The inner void and the tube walls are visible in the TEM images and show the typical dimensions of TNTs. As expected, the tubes are strongly bundled. For imaging, the end of a bundle was chosen where the individual tubes start to separate. The nanotubes depicted in Fig. 8 seem to be of multiwall type with two walls.

IV. DISCUSSION

A. Chemical and structural properties of carbothermally treated titania (precursor powder)

Commercially available titania powder (P25) was treated carbothermally in the temperature range of 700–1050 °C in acetylene/nitrogen flow. The resulting material was investigated regarding phase content, carbon content, and morphology.

B. Pretreatment temperatures 700–800 °C

XRD investigations reveal that the phase content is identical with that of untreated titania (CP0) for treatment temperatures of 700 °C (CP7) and 800 °C (CP8). The untreated TiO_2 powder consists of anatase and rutile. Mild reaction conditions under reducing atmosphere do not change the phase content as it is detectable within the limits of XRD. However, significant carbon content of about 9–29 wt% was measured by TGA-FTIR for samples CP7 and CP8, respectively. Due to the absence of the crystalline carbon phase in our XRD patterns, we suggest that the carbon in samples CP7 and CP8 is mainly present as amorphous carbon. We suppose that the amorphous carbon is located on the powder particles, possibly as a shell. The assumption is supported by the absence of grain coarsening, which is validated by SEM and BET results. Such shells around titania grains were reported in Ref. 16 by Huang et al. The authors demonstrated that after 20 min in acetylene–nitrogen gas mixture at 700 °C, pure titania P25-powder was coated with a uniform amorphous carbon shell (≈5 nm), which was not detectable by XRD and which also prevented severe sintering of titania grains. Furthermore, our experiments showed that below 900 °C, phase content regarding the titanium dioxide polymorph did not change with temperature treatment although the transformation of anatase to rutile could be expected. It is well established that for fine titania powders, the formation of rutile occurs around 600–700 °C since rutile is the thermodynamically stable phase.[32] However, in our

https://doi.org/10.1557/jmr.2018.49 Published online by Cambridge University Press

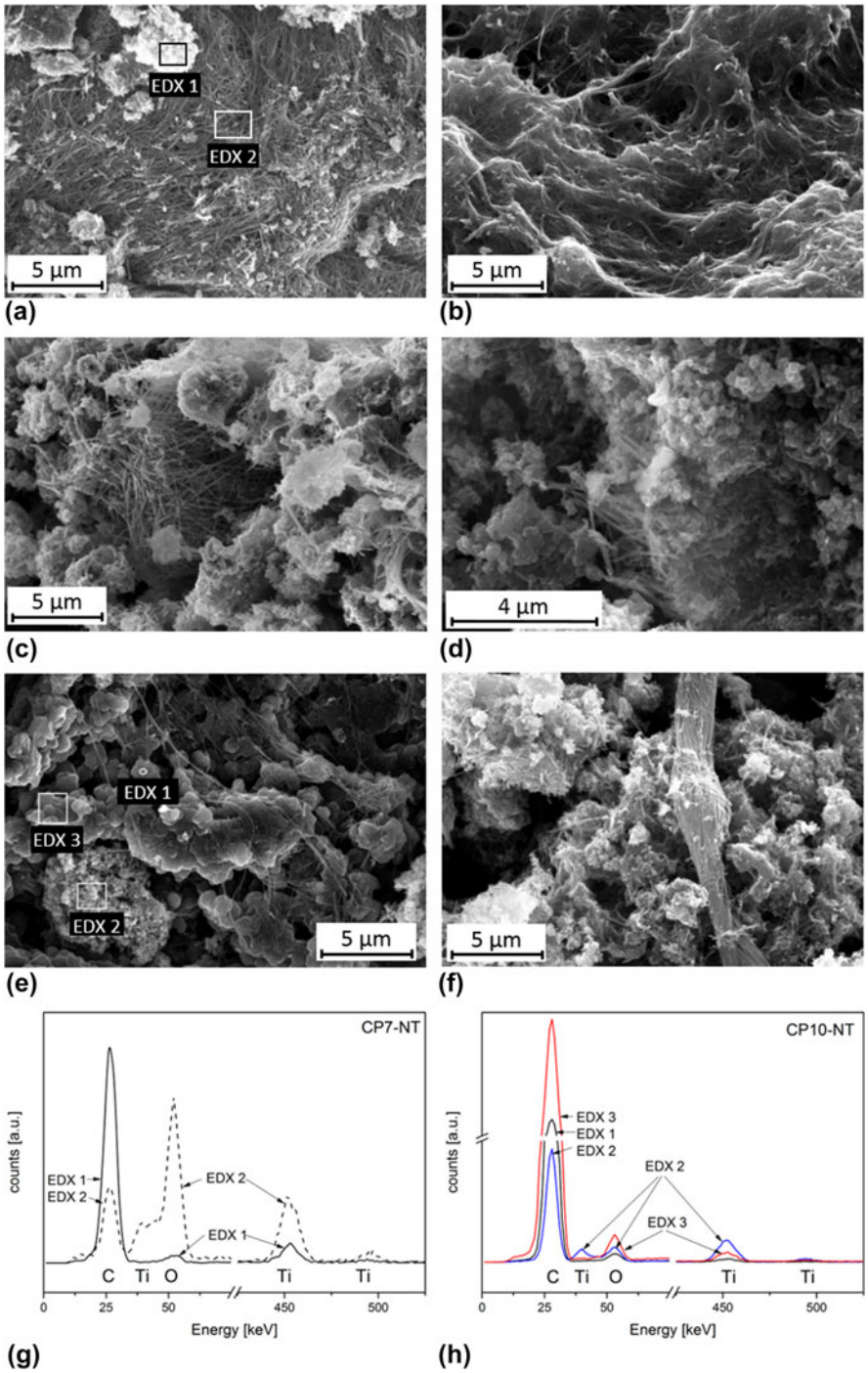


FIG. 7. SEM images and EDX plots of carbon-doped TNTs. (a) CP7-NT, (b) CP8-NT, (c) CP9-NT, (d) CP9.5-NT, (e) CP10-NT, (f) CP10.5-NT (modified after[19]), (g) EDX spectra of sample CP7-NT, and (h) EDX spectra of sample CP10-NT.

experiments, the amount of rutile does not increase upon thermal treatment. This observation further supports the postulation of an amorphous carbon shell. It is frequently reported that the anatase to rutile transformation is shifted to temperatures above 900 °C due to the presence of carbon coating,[16,33] a carbon containing atmosphere,[34] or carbon aerogels.[35] The mechanism behind the shift in the transformation temperature is not yet identified in the literature and needs further investigation. The inhibition of rutile crystallization during carbothermal treatment of titania can be beneficial for a high-yield synthesis of carbon-doped TNTs because rutile shows slower dissolution-kinetics during hydrothermal synthesis than anatase.[36]

https://doi.org/10.1557/jmr.2018.49 Published online by Cambridge University Press

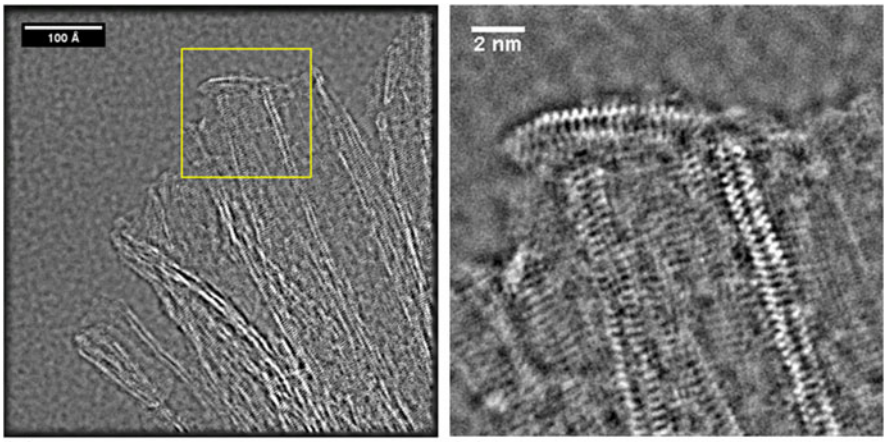


FIG. 8. TEM micrographs. (a) Bundle of carbon-doped TNTs (CP7-NT) which were synthesized from titania powder pretreated at 700 °C (CP7) and (b) detailed TEM micrograph of (a) showing the tube walls.

The carbon content significantly increases from 9 to 29 wt% for the samples CP7 and CP8. The increase with the reaction temperature can be ascribed to a higher yield of carbon, due to higher reaction rates of acetylene decomposition.[37,38]

C. Pretreatment temperatures 900–1050 °C

Above 900 °C, we observe several substoichiometric titanium oxides (suboxides) starting with Ti_9O_{17} at 900 °C (CP9) followed by mixtures of Ti_4O_7, Ti_3O_5, and titanium oxycarbide in samples CP9.5–CP10.5. Suboxides with the general formula Ti_nO_{2n-1}, also known as Magnéli phases,[39] are formed in reducing atmosphere from titania. The titanium to oxygen ratio is dependent on the degree of reduction which is mainly determined by the reducing environment, particle size, packing density, temperature profile, and reduction duration.[40] With the increasing temperature, the titanium to oxygen ratio increases.[41,42] Our results from the XRD measurements correspond to the observations reported in the literature. The highest reaction temperatures applied lead to products with the highest titanium to oxygen ratio, i.e., to oxycarbides. Titanium oxycarbides are phases within the solid solution of TiO and TiC with the general formula TiO_xC_{1-x}[43] and complete miscibility. It was shown by in situ XPS measurements in carbon containing reducing atmosphere that TiO_xC_{1-x} is formed via intermediate titanium suboxides, by replacing oxygen vacancies with carbon atoms.[44] The process is time-dependent, where the suboxide phase is converted into TiO_xC_{1-x} with prolonged reduction duration.[41] Considering that the carbothermal treatment in our experiments was rather short (10 min), it is reasonable that we observe a mixture of anatase, TiO_xC_{1-x}, and suboxides due to an incomplete conversion. For example, Koc et al. obtained a mixture of Ti_3O_5 and TiO_xC_{1-x} after a 2-h reduction of carbon-coated P25 titania powder at 1200 °C,[45] whereas Huang et al. report the formation of pure TiO_xC_{1-x} from carbon-coated P25 titania after a reduction of 4 h.[16]

D. TNTs from carbon-doped precursor powders

XRD patterns and TEM investigations proved that TNTs were obtained from the pretreated carbon containing titania powder. After hydrothermal treatment, the characteristic peaks for TNTs were observed. SEM investigation shows elongated structures in all samples beside agglomerated powder particles in different amounts. TEM images prove that the sample synthesized from titania treated carbothermally at 700 °C contains tubular morphologies typical for TNTs.

In addition to structure and morphology investigations, the specific surface area measured via nitrogen adsorption was taken as a measure for the amount of nanotube formation. The reference point for our experiments was the specific surface area of undoped nanotube samples synthesized in our laboratory. We achieved 380 m^2/g for the reference nanotube sample (CP0-NT) which is in good agreement with the literature studies.[46,46–48] In comparison, values between 340 m^2/g (CP7-NT) and 175 m^2/g (CP10.5-NT) were obtained for the samples synthesized from carbothermally pretreated titania powders (CP7-10.5). It is noteworthy to mention that for all samples, the specific surface area is significantly higher than that measured at pretreated powder samples which varies around 45–55 m^2/g. The high specific surface area can be taken as indication for the successful transformation of at least part of the precursor powder into nanotubes. The presence of nanotubes in the sample CP7-NT was proven using TEM. Tube walls and the inner void are clearly visible. Not all samples could be investigated by TEM so that the information about the morphology of the nanomaterial can be drawn only from SEM investigations and specific surface area measurements. However, both methods support the assumption that also in the

https://doi.org/10.1557/jmr.2018.49 Published online by Cambridge University Press

samples synthesized from precursor powders treated at higher temperatures, nanotubes were formed. SEM investigations show the presence of elongated structures beside agglomerated powder particles. However, from the images only, it is not possible to decide whether the elongated structures are nanotubes or nanofibers. A first hint is that nanofibers are usually observed after hydrothermal treatment at temperatures higher than 170 °C.[11] Additionally, the value for the specific surface area points toward nanotubes. Geometrical considerations assuming ideal morphology lead to simple correlation between specific surface area, diameter, and wall thickness, respectively.[11] The following equations can be derived (neglecting the end surfaces):

$$S = \frac{4}{\rho d} \quad \text{for nanofibers} \quad , \tag{1}$$

where S = specific surface area, ρ = density, d = diameter and:

$$S = \frac{2}{\rho h} \quad \text{for nanotubes} \quad , \tag{2}$$

where h = wall thickness (for more complete equations, see the Supplementary Material).

Please note that the specific surface area of the tubes is only dependent on the wall thickness, which for the titanium oxide tubes is around 2 nm.

Following Bavykin and Walsh,[11] the density was assumed to be 3.16 g/cm^3. Assuming that the whole sample consists of nanotubes, a wall thickness of 1.86 nm is calculated for CP7-NT after Eq. (2). The value corresponds well to that estimated from TEM investigations. The samples CP8-NT to CP10.5-NT show lower specific surface areas. The lowest value measured was 175 m^2/g. Calculating a wall thickness based on that value using Eq. (2) leads to 3.62 nm which is still reasonable for TNTs. Assuming that the elongated structures are nanowires without inner voids, reveals a diameter of 7.23 nm following Eq. (1). However, typical diameters of titanate nanofibers range between 20 and 200 nm. Furthermore, the samples consist also of larger powder particles which contribute much lower to the specific surface area. Summarizing all these considerations, it is plausible to state that also from precursor powders pretreated at temperatures above 700 °C, nanotubes are formed beside residual precursor powder.

As described in the results section, the specific surface area of the nanotube samples decreases with increasing pretreatment temperature of the precursor powder (Table I). Additionally, a lower amount of adsorbed water is observed. Both results indicate that at higher pretreatment temperature, the formation of titanium nanotubes was partially suppressed in favor of other phases. The assumption is further supported by the SEM images and the phase analysis.

As mentioned above, with increasing pretreatment temperature, a higher fraction of agglomerated powder particles is observed beside elongated structures. EDX investigations show that the relative amount of carbon in the particle fraction is higher than in the fibrous regions. Although the interpretation of the measurement data is difficult due to carbon sputtering of the samples prior to SEM investigations, the comparison of the signal intensities suggests that a high amount of carbon is retained in the particle fraction. Simultaneously, the XRD measurement shows the presence of rutile and an increasing amount of titanium oxycarbides with increasing pretreatment temperatures. We assume that the nontubular fraction is mainly residual titanium oxycarbide and rutile not reacted during the hydrothermal treatment. The assumption is supported by investigations regarding the stability of TiC in several corrosive media.[49] The authors report that TiC is inert against strong aqueous bases such as NaOH. Among the possible titanium oxide phases, rutile is most stable against dissolution during hydrothermal treatment.[36] Other titanium oxide phases such as anatase or titanium monoxide are less stable or even soluble in aqueous media and disappear during hydrothermal treatment.

From those observations, we conclude that carbothermal treatment of titania powders at temperatures below 800 °C is most suitable for the synthesis of carbon-doped TNTs among the conditions tested. Criteria for optimum synthesis parameters are high yield and high specific surface area of the tubular products obtained.

The question whether carbon doping of the tubes was successful is not easy to answer from the data we obtained. Several observations point toward carbon incorporation into the tubes:

(i) The overall carbon content of the nanotube samples increases from 6.0 wt% (pretreatment temperature 700 °C) to 43.5 wt% (pretreatment temperature 1050 °C).

(ii) All samples show the same carbon content before and after hydrothermal treatment within the error limits (Table II).

(iii) The mass loss during thermal analysis which could be correlated with carbon degradation, occurs at temperatures only above 380 °C which suggests strong bonding of carbon within the structure.

Further investigation using spectroscopic methods, especially XPS and AC impedance spectroscopy could

TABLE II. Carbon content in wt% of precursor powders and carbon-doped TNTs (C-TNTs) in dependence of powder pretreatment temperature.

Temperature [°C]	700	800	900	950	1000	1050
Precursor powder	8.9	29.4	41.4	45	38.3	42.8
C-TNTs	6.0	20.9	36.7	40.3	43.1	43.5

https://doi.org/10.1557/jmr.2018.49 Published online by Cambridge University Press

give further insight into the nature of carbon incorporation into the material.

However, our investigations clearly demonstrate that TNTs with high specific surface area (340 m^2/g) can be synthesized from carbothermally treated titania precursor powder (700 °C). It is noteworthy to mention that the samples contain a significant amount of carbon (6 wt%). Although the nature of carbon incorporation could not be clarified, the experiments open a new path toward tubular nanostructures from titanium oxide avoiding posttreatment which is known to destroy the nanotube morphology.

V. SUMMARY AND CONCLUSION

A new method for the fabrication of carbon-doped TNTs was investigated. The hydrothermal method was modified replacing the untreated titania powder starting material by carbon-doped titania powders obtained via carbothermal treatment in acetylene/nitrogen flow. All samples were characterized by means of XRD, SEM, BET, and TGA. After hydrothermal treatment, the reaction products were additionally analyzed by TEM. Below 900 °C, carbothermal treatment of titania does not change the phase content significantly, while the carbon content increases from about 9 wt% (700 °C) to about 21 wt% (800 °C). From 900 °C to 1050 °C, various substoichiometric titanium oxides and titanium oxycarbides are formed with a maximum carbon content of about 43 wt%. Nanotubes with high specific surface area (340 m^2/g) were successfully formed via hydrothermal treatment. Carbon content in the samples could be proved although the type of incorporation could not be clarified.

It was shown that carbon is incorporated in the new precursor powder. After treatment at 700 °C, the precursor powder consists of anatase and rutile. About 9 wt% carbon is incorporated into the powder, presumably as amorphous carbon coating. Such precursor powder was successfully transformed into TNTs with high specific surface area (340 m^2/g), 6 wt% carbon, and a low amount of by-products. Higher pretreatment temperatures lead to the formation of titanium suboxides and titanium oxycarbides in the precursor powders with a carbon content up to about 43 wt%. After hydrothermal treatment of such powders, a higher amount of unreacted agglomerates beside tubular structures is observed.

The carbon content in the precursor powders and the hydrothermally treated material is comparable. The precise amount of carbon incorporated into the nanotube structure and the exact location of the carbon atoms remain unclear and should be subject of further investigations. First investigations of the electrical conductivity of carbon-doped precursor powders and carbon-doped TNTs show a significant influence of the carbothermal pretreatment. This behavior will be examined by AC impedance spectroscopy in further studies.

ACKNOWLEDGMENT

The authors thank the German Research Foundation (DFG) for financial support (GZ: HE 7821/1-1, Projektakademie Ingenieurwissenschaften).

REFERENCES

1. X. Sun and Y. Li: Synthesis and characterization of ion-exchangeable titanate nanotubes. *Chem. – Eur. J.* **9**, 2229 (2003).
2. D.V. Bavykin, K.E. Redmond, B.P. Nias, A.N. Kulak, and F.C. Walsh: The effect of ionic charge on the adsorption of organic dyes onto titanate nanotubes. *Aust. J. Chem.* **63**, 270 (2010).
3. D.V. Bavykin, J.M. Friedrich, and F.C. Walsh: Protonated titanates and TiO_2 nanostructured materials: Synthesis, properties, and applications. *Adv. Mater.* **18**, 2807 (2006).
4. D.V. Bavykin and F.C. Walsh: Elongated titanate nanostructures and their applications. *Eur. J. Inorg. Chem.* **2009**, 977 (2009).
5. H. Ou and S. Lo: Review of titania nanotubes synthesized via the hydrothermal treatment: Fabrication, modification, and application. *Sep. Purif. Technol.* **58**, 179 (2007).
6. V. Štengl, S. Bakardjieva, J. Šubrt, E. Večerníková, L. Szatmary, M. Klementová, and V. Balek: Sodium titanate nanorods: Preparation, microstructure characterization and photocatalytic activity. *Appl. Catal., B* **63**, 20 (2006).
7. M. Paulose, H.E. Prakasam, O.K. Varghese, L. Peng, K.C. Popat, G.K. Mor, T.A. Desai, and C.A. Grimes: TiO_2 nanotube arrays of 1000 μm length by anodization of titanium foil: Phenol red diffusion. *J. Phys. Chem. C* **111**, 14992 (2007).
8. T. Kasuga, M. Hiramatsu, A. Hoson, T. Sekino, and K. Niihara: Formation of titanium oxide nanotube. *Langmuir* **14**, 3160 (1998).
9. S.K. Pradhan, Y. Mao, S.S. Wong, P. Chupas, and V. Petkov: Atomic-scale structure of nanosized titania and titanate: Particles, wires, and tubes. *Chem. Mater.* **19**, 6180 (2007).
10. N. Liu, X. Chen, J. Zhang, and J.W. Schwank: A review on TiO_2-based nanotubes synthesized via hydrothermal method: Formation mechanism, structure modification, and photocatalytic applications. *Catal. Today* **225**, 34 (2014).
11. D.V. Bavykin and F.C. Walsh: *Titanate and Titania Nanotubes* (Royal Society of Chemistry, Cambridge, 2009).
12. D.C.B. Alves, F.C. Fonseca, F.D. Brandão, K. Krambrock, and A.S. Ferlauto: Temperature dependence of the electrical properties of hydrogen titanate nanotubes. *J. Appl. Phys.* **116**, 184307 (2014).
13. W. Hu, L. Li, G. Li, J. Meng, and W. Tong: Synthesis of titanate-based nanotubes for one-dimensionally confined electrical properties. *J. Phys. Chem. C* **113**, 16996 (2009).
14. Y. Kado, R. Hahn, and P. Schmuki: Surface modification of TiO_2 nanotubes by low temperature thermal treatment in C_2H_2 atmosphere. *J. Electroanal. Chem.* **662**, 25 (2011).
15. R. Hahn, A. Ghicov, J. Salonen, V-P. Lehto, and P. Schmuki: Carbon doping of self-organized TiO_2 nanotube layers by thermal acetylene treatment. *Nanotechnology* **18**, 105604 (2007).
16. K. Huang, Y. Li, and Y. Xing: Carbothermal synthesis of titanium oxycarbide as electrocatalyst support with high oxygen evolution reaction activity. *J. Mater. Res.* **28**, 454 (2013).
17. R. Hahn, F. Schmidt-Stein, J. Salonen, S. Thiemann, Y. Song, J. Kunze, V-P. Lehto, and P. Schmuki: Semimetallic TiO_2 nanotubes. *Angew. Chem., Int. Ed. Engl.* **48**, 7236 (2009).
18. F. Schmidt-Stein, S. Thiemann, S. Berger, R. Hahn, and P. Schmuki: Mechanical properties of anatase and semi-metallic TiO_2 nanotubes. *Acta Mater.* **58**, 6317 (2010).
19. K. Herbst: Elektrisch leitfähige Ti–O–C–Nanotubes mit hoher spezifischer Oberfläche: (Electrically conductive Ti–O–C nanotubes with high specific surface area. -in German-). Dissertation, Friedrich-Alexander-University Erlangen-Nuremberg, Erlangen, Germany, 2015.

https://doi.org/10.1557/jmr.2018.49 Published online by Cambridge University Press

20. M. Zhang, Z. Jin, J. Zhang, X. Guo, J. Yang, W. Li, X. Wang, and Z. Zhang: Effect of annealing temperature on morphology, structure and photocatalytic behavior of nanotubed $H_2Ti_2O_4(OH)_2$. *J. Mol. Catal. A: Chem.* **217**, 203 (2004).
21. E. Morgado, M.A. de Abreu, O.R. Pravia, B.A. Marinkovic, P.M. Jardim, F.C. Rizzo, and A.S. Araújo: A study on the structure and thermal stability of titanate nanotubes as a function of sodium content. *Solid State Sci.* **8**, 888 (2006).
22. Z. Wu, F. Dong, W. Zhao, H. Wang, Y. Liu, and B. Guan: The fabrication and characterization of novel carbon doped TiO_2 nanotubes, nanowires and nanorods with high visible light photocatalytic activity. *Nanotechnology* **20**, 235701 (2009).
23. A. Ansón-Casaos, I. Tacchini, A. Unzue, and M.T. Martínez: Combined modification of a TiO_2 photocatalyst with two different carbon forms. *Appl. Surf. Sci.* **270**, 675 (2013).
24. J. Xu, Y. Wang, Z. Li, and W.F. Zhang: Preparation and electrochemical properties of carbon-doped TiO_2 nanotubes as an anode material for lithium-ion batteries. *J. Power Sources* **175**, 903 (2008).
25. E.M. Neville, J.D. MacElroy, K.R. Thampi, and J.A. Sullivan: Visible light active C-doped titanate nanotubes prepared via alkaline hydrothermal treatment of C-doped nanoparticulate TiO_2: Photo-electrochemical and photocatalytic properties. *J. Photochem. Photobiol., A* **267**, 17 (2013).
26. S. Goriparti, E. Miele, M. Prato, A. Scarpellini, S. Marras, S. Monaco, A. Toma, G.C. Messina, A. Alabastri, F. de Angelis, L. Manna, C. Capiglia, and R.P. Zaccaria: Direct synthesis of carbon-doped TiO_2-bronze nanowires as anode materials for high performance lithium-ion batteries. *ACS Appl. Mater. Interfaces* **7**, 25139 (2015).
27. M. Lehmann: Determination and correction of the coherent wave aberration from a single off-axis electron hologram by means of a genetic algorithm. *Ultramicroscopy* **85**, 165 (2000).
28. I.M. Pohrelyuk, O.I. Yas'kiv, V.M. Fedirko, and S.V. Huryn: Laws of formation of oxycarbide layers on titanium in carbon- and oxygen-containing media. *Mater. Sci.* **39**, 400 (2003).
29. Y. Tang, Y. Zhang, J. Deng, J. Wei, H. Le Tam, B.K. Chandran, Z. Dong, Z. Chen, and X. Chen: Mechanical force-driven growth of elongated bending TiO_2-based nanotubular materials for ultrafast rechargeable lithium ion batteries. *Adv. Mater.* **26**, 6111 (2014).
30. J. Yang, Z. Jin, X. Wang, W. Li, J. Zhang, S. Zhang, X. Guo, and Z. Zhang: Study on composition, structure and formation process of nanotube $Na_2Ti_2O_4(OH)_2$. *Dalton Trans.* **20**, 3898 (2003).
31. A-L. Papa, N. Millot, L. Saviot, R. Chassagnon, and O. Heintz: Effect of reaction parameters on composition and morphology of titanate nanomaterials. *J. Phys. Chem. C* **113**, 12682 (2009).
32. D.A.H. Hanaor and C.C. Sorrell: Review of the anatase to rutile phase transformation. *J. Mater. Sci.* **46**, 855 (2011).
33. T. Tsumura, N. Kojitani, I. Izumi, N. Iwashita, M. Toyoda, and M. Inagaki: Carbon coating of anatase-type TiO_2 and photoactivity. *J. Mater. Chem.* **12**, 1391 (2002).
34. C.S. Enache, J. Schoonman, and R. van de Krol: Addition of carbon to anatase TiO_2 by *n*-hexane treatment—Surface or bulk doping? *Appl. Surf. Sci.* **252**, 6342 (2006).
35. Q. Meng, X. Li, L. Liu, and B. Cao: High-temperature preparation and electrochemical properties of TiO_2 anatase phase-mounted carbon aerogels. *J. Mater. Sci.* **47**, 5926 (2012).
36. D.L. Morgan, G. Triani, M.G. Blackford, N.A. Raftery, R.L. Frost, and E.R. Waclawik: Alkaline hydrothermal kinetics in titanate nanostructure formation. *J. Mater. Sci.* **46**, 548 (2011).
37. M.H. Khedr, K.S. Abdel Halim, and N.K. Soliman: Effect of temperature on the kinetics of acetylene decomposition over reduced iron oxide catalyst for the production of carbon nanotubes. *Appl. Surf. Sci.* **255**, 2375 (2008).
38. G.D. Towell and J.J. Martin: Kinetic data from nonisothermal experiments: Thermal decomposition of ethane, ethylene, and acetylene. *AIChE J.* **7**, 693 (1961).
39. S. Andersson and A. Magnéli: Diskrete Titanoxydphasen im Zusammensetzungsbereich $TiO_{1,75}$–$TiO_{1,90}$. *Naturwissenschaften* **43**, 495 (1956).
40. F.C. Walsh and R. Wills: The continuing development of Magnéli phase titanium sub-oxides and Ebonex® electrodes. *Electrochim. Acta* **55**, 6342 (2010).
41. M.A. Dewan, G. Zhang, and O. Ostrovski: Carbothermal reduction of titania in different gas atmospheres. *Metall. Mater. Trans. B* **40**, 62 (2009).
42. W. Sen, B-q. Xu, B. Yang, H-y. Sun, J-x. Song, H-l. Wan, and Y-n. Dai: Preparation of TiC powders by carbothermal reduction method in vacuum. *Trans. Nonferrous Met. Soc. China* **21**, 185 (2011).
43. B. Jiang, N. Hou, S. Huang, G. Zhou, J. Hou, Z. Cao, and H. Zhu: Structural studies of $TiC_{1-x}O_x$ solid solution by Rietveld refinement and first-principles calculations. *J. Solid State Chem.* **204**, 1 (2013).
44. L. Calvillo, D. Fittipaldi, C. Rüdiger, S. Agnoli, M. Favaro, C. Valero-Vidal, C. Di Valentin, A. Vittadini, N. Bozzolo, S. Jacomet, L. Gregoratti, J. Kunze-Liebhäuser, G. Pacchioni, and G. Granozzi: Carbothermal transformation of TiO_2 into TiO_xC_y in UHV: Tracking intrinsic chemical stabilities: Tracking intrinsic chemical stabilities. *J. Phys. Chem. C* **118**, 22601 (2014).
45. R. Koc and J.S. Folmer: Carbothermal synthesis of titanium carbide using ultrafine titania powders. *J. Mater. Sci.* **32**, 3101 (1997).
46. S. Mozia, E. Borowiak-Paleń, J. Przepiórski, B. Grzmil, T. Tsumura, M. Toyoda, J. Grzechulska-Damszel, and A.W. Morawski: Physico-chemical properties and possible photocatalytic applications of titanate nanotubes synthesized via hydrothermal method. *J. Phys. Chem. Solids* **71**, 263 (2010).
47. C-C. Tsai and H. Teng: Regulation of the physical characteristics of titania nanotube aggregates synthesized from hydrothermal treatment. *Chem. Mater.* **16**, 4352 (2004).
48. N. Wang, H. Lin, J. Li, X. Yang, B. Chi, and C. Lin: Effect of annealing temperature on phase transition and optical property of titanate nanotubes prepared by ion exchange approach. *J. Alloys Compd.* **424**, 311 (2006).
49. H.W. Philipp: *Chemical Reactions of Carbides, Nitrides, and Diborides of Titanium and Zirconium and Chemical Bonding in these Compounds* (NASA TN, Washington, D.C., 1966); p. 1.

Supplementary Material

To view supplementary material for this article, please visit https://doi.org/10.1557/jmr.2018.49.

https://doi.org/10.1557/jmr.2018.49 Published online by Cambridge University Press